University of North Carolina Asheville
Journal of Undergraduate Research
Asheville, North Carolina
Spring 2024

Aspects of Gigantic-Jet Producing Thunderstorms in Different Environments

Evan Johnson

Atmospheric Sciences

The University of North Carolina Asheville

One University Heights

Asheville, North Carolina 28804 USA

Faculty Mentor: Dr. Elaine Godfrey

Abstract

Gigantic jets (GJs) represent a type of upper atmospheric lightning within the broader family of transient luminous events, often extending up from the cloud top to the lower ionosphere. Given the rarity of GJ events, their impact on the global electric circuit and the surrounding environment remains fairly unknown, as is the impact of GJs on the electrical nature of thunderstorms, and consequently on lightning within them. In general, a comprehensive understanding of lightning within thunderstorms can help forecasters and residents prepare for potentially damaging events initiated by lightning. Perhaps, as a few researchers have suggested, the GJ-producing thunderstorm environment could allow for insight into when and where GJs occur and their associated repercussions. Few studies have explored GJs in significantly different environments. The research presented here uses model reanalysis data to describe GJ-producing thunderstorms by investigating different atmospheric variables, such as CAPE and equivalent potential temperature, in varying environments. This study also utilizes radar data to examine the structure of storms from several case studies. The analysis will not only describe characteristics of the GJ-producing thunderstorm but also equip future researchers with a diagnostic tool for identifying GJ storms and the lightning within them.

1. Introduction

Gigantic jets (GJs) represent a type of upward lightning that forms in various conditions, extending from the cloud top to the lower ionosphere. Due to the rarity of GJ events, their impact on the global electric circuit and the surrounding environment has yet to be established. Furthermore, the impact of GJs on the electrical nature of thunderstorms, and consequently on the lightning within them, while a subject under intense study, remains relatively unknown. In general, a comprehensive understanding of lightning within thunderstorms can help forecasters and residents prepare for potentially damaging events initiated by lightning. The first exploration of GJs and their impacts, done by Pasko et al. (2002) and Su and Coauthors (2003), serves as an inspiration for many future research articles. The GJ observed by Pasko et al. (2002) occurred on 14 September, 2001 at approximately 0325 UTC northwest of the Arecibo Observatory in Puerto Rico and reached an altitude of about 70 km. Su and Coauthors (2003) investigated five South China Sea GJ observations, suggesting they should be added to the global electrical circuit. These articles hold significance in the history of GJ observations, despite lacking a detailed meteorological synopsis of the storms that produced the GJs.

A more in-depth analysis of a continental GJ storm written by van der Velde et al. (2007) gives a thorough exploration of lightning activity in relation to the GJ and a radar analysis of the storm. While this does provide a comprehensive study on a continental GJ storm, it does not look at the environment that produced the storm. Peering into the environment of a storm allows researchers to further identify the type of storms that may produce GJs. Another investigation into a Northern Hemisphere winter 2009 GJ-producing storm conducted by van der Velde and Coauthors (2010) offers the meteorological context behind the storm — noteworthy because of the storm's environment and characteristics. This thunderstorm had a cloud top of only about 6.5 km and brightness temperatures of -34 °C. The brightness temperature is about half of previously reported GJ thunderstorms. More recent studies after van der Valde and Coauthors (2010) emphasize both the structure of the GJ and the meteorological context (environment) behind the storm.

Work by Meyer et al. (2013) analyzed the environment, structure, and evolution of six GJ-producing storms. They saw that even though the GJ-producing storms formed in different locations (over land or water), there were no obvious differences in environmental parameters or storm characteristics. For example, a GJ-producing storm off the coast of Florida (CAPE of 2473 J kg^{-1}) had very similar environmental characteristics to a storm over land in Oklahoma (CAPE of 2344 J kg^{-1}). This study also made the important distinction that GJ storms often occur with over-shooting cloud tops. Furthermore, they indicated that for five out of six GJ cases, the GJ occurred as the storm underwent a convective surge (a period of rapid development) or had just undergone a convective surge. The foundational work of Meyer et al. (2013) connects multiple case studies and the environment of each storm into a common thread.

Lazarus et al. (2015) conducted an in-depth analysis of a GJ-producing August 2013 Florida thunderstorm, examining parameters like CAPE, storm top turbulence and mixing, and wind shear to characterize the storm. This article categorized past GJ events

into moderate and high shear events, acting as a useful interpretation of the environmental variables by connecting the events together and identifying outliers. The authors also explore lightning characteristics and the microphysical aspects of the Florida thunderstorm, which they observed near tropical depression Dorian after it rapidly reintensified. Lazarus et al. (2021) also investigated Dorian when examining the meteorological attributes of three GJ producing tropical cyclones and three oceanic thunderstorms not associated with GJs. This study's key finding revealed that the tropical cyclone GJ environment typically featured colder brightness temperatures (higher cloud tops correlate with colder temperatures), a higher tropopause, and a more stable lower stratosphere. The results in this paper hold significance, as they establish a benchmark for oceanic and tropical cyclone GJ environments, which researchers may utilize in future studies.

In another study, conducted by van der Velde et al. (2022), ERA5 reanalysis data is harnessed to investigate both GJ-producing storms and non-GJ storms. Furthermore, the paper provides a climatology of GJs and the environments within GJ-producing storms in Colombia. Their findings unveil a robust statistical performance of parameters related to warm cloud depth and condensation. When combining temperature difference (between mid-levels in GJ storms and null cases) and the LCL height, they noticed an improvement in the GJ and null case separation. They also found a smaller distance between the -10 °C and -50 °C isotherms during nights when GJs formed. These results are significant as they provide a proxy for understanding the thunderstorm environment behind GJ storms with a specific parameter. The authors suggest that by studying reanalysis or forecast maps of this isotherm parameter, “it may be understood better how weather systems create a favorable environment for GJ-producing storms” (van der Velde et al. 2022). An interesting note is that the hypothesis suggested by Lazarus et al. (2015) regarding the prevalence of vertical wind shear and overshooting cloud tops did not align with the results of van der Velde et al. (2022).

These discrepancies suggest a lack of knowledge on the environments conducive to GJ-producing thunderstorms. Another inconsistency presented by van der Velde and Coauthors (2010), a low CAPE winter GJ-producing thunderstorm, also provides evidence of a general unfamiliarity with GJ storm environments. This research aims to fill in the gap of knowledge by utilizing ERA5 reanalysis data while addressing inconsistencies found in previous results. Furthermore, this paper presents the characteristics of at least three different case studies of GJ-producing thunderstorms in different environments. Each case study involves the analysis of multiple variables, including CAPE and equivalent potential temperature. Radar and satellite data also contribute to the analysis for each case study. By combining ERA5 reanalysis, radar, and satellite data, this research provides a more comprehensive look at specific GJ thunderstorm environments. Given the rarity of GJ observations, most of the cases chosen from previous papers undergo consideration from another perspective. In summary, this research endeavors to bridge the gaps in the understanding of GJ-producing thunderstorms by analyzing the dynamic and thermo-dynamic characteristics of their environments. Moreover, the analysis here equips future researchers with a diagnostic tool for identifying GJ storms and the lightning within them.

2. Data and Methods

2.1 ERA5 Reanalysis Data

The primary analysis of GJ pre-storm environments used the Copernicus Climate Change Service ERA5 reanalysis dataset (Hersbach and Coauthors 2020). ERA5, the fifth-generation global reanalysis from ECMWF, has data from 1940 onwards. The specific datasets used in case studies consist of hourly data on multiple pressure levels and surface (single level) data. Pressure level reanalysis data has a vertical coverage from 1000 hPa to 1 hPa. Both single level data and pressure level data have horizontal resolution (latitude-longitude grid spacing) of 0.25° with a vertical resolution of 37 pressure levels. This study only utilizes data from 1000 hPa to 20 hPa, because all of the GJ-storm cloud tops occur below 20 hPa.

Because of underground 1000 hPa data levels, geopotential data are used to calculate the approximate height of the surface at a specific date and time. For example, the surface in the Kansas GJ cases (Storm A from Table 1) was above 1000 hPa, at around 920 hPa, depending on the location of the sounding. The data corresponding with the actual surface pressure and height (2m temperature, dewpoint, 10m winds, etc.) from the single level dataset replaced data below the actual height of the surface. The opposite scenario occurred in the Florida GJ cases (Storm B from Table 1). The surface was below 1000 hPa, so the corresponding data at the surface (at approximately 1016 hPa), was added on to the pressure level data. One potential downfall of using the ERA5 dataset can be seen in the coarse horizontal resolution. The analysis presented in this paper relies on storm-scale processes, which happen on a smaller scale (higher resolution) than the output data from ERA5. A sounding picked at the nearest grid point accounted for this issue. All results depict a pre-convection environment (before the storm arrived or formed), in order to best account for the environment that allowed for the GJ-producing thunderstorm.

2.2 Radar and Satellite Data

This study also utilized radar and satellite data to examine each storm during and after convection. Radar data comes from the National Centers for Environmental Information (NCEI) NEXRAD database. Satellite data obtained from the Amazon Web Services (AWS) open database for the NOAA Geostationary Operational Environmental Satellites series (GOES) 16, 17, and 18 (see data availability statement). NOAA also provides the Comprehensive Large Array-data Stewardship System (CLASS) for use (see data availability statement). The satellite imagery data provided by CLASS goes back to GOES-08.

The Man–Computer Interactive Data System (McIDAS; see online at https://www.ssec.wisc.edu/mcidas/software/), a data visualization software package developed by the Space Science and Engineering Center (SSEC) at the University of Wisconsin–Madison has a Range Height Indicator (RHI) cross section option when

working with radar data. RHI mode keeps the azimuth angle of the radar constant, while changing the elevation angle. Therefore, one can obtain a vertical cross section of the radar imagery. The azimuth angle pertaining to the GJ location on the radar scan was found in McIDAS-V, while the RHI plots and Planned Position Indicator (PPI) plots of radar were created using the Python ARM Radar Toolkit (Py-ART, see Helmus and Collis 2016).

One problem with analyzing radar and satellite data seen in this study has to do with the temporal resolution. Radar scans approximately every 5 minutes, while satellite data has a temporal resolution of approximately 10 minutes. Each of the GJs occurred at a time that was not scanned by the radar or available through satellite imagery. To fix this problem, the analysis of each GJ corresponds to the nearest time of the radar or satellite imagery. For example, the first Kansas GJ occurred at exactly 04:03:55 UTC, but the closest radar scan was at 04:02:07 UTC.

3. Results

The three GJ producing storms analyzed consisted of two over water, and one over land. Storms A and C occurred over land, while storm B occurred over water (see Table 1).

Date	Time of GJ (UTC)	Storm Letter	Event #	Location	Latitude	Longitude	Polarity	Paper
06/13/2022	04:03:55	A	1	Land	39.1591	-99.7021	+	N/A
	04:10:52	A	2		39.3174	-99.5115	+	
	05:01:47	A	3		39.4315	-98.8638	+	
08/03/2013	03:54:12.833	B	1	Water	27.8804	-79.8948	-	Lazarus et. al., 2015
	03:56:55.530	B	2		27.9494	-79.8438	-	
	03:58:21.933	B	3		27.9388	-79.8348	-	
	04:11:38.667	B	4		27.9235	-79.8818	-	
05/13/2005	04:23:50	C	1	Land	28.7	-101.5	-	van der Velde, et. al. 2007

Table 1. Table of three GJ-producing storms covered in this paper, including the date, UTC time, location, electrical polarity of the GJ, and the paper analyzing the GJ.

3.1 Kansas GJ-producing storm (Storm A)

This storm produced three positive GJs, each occurring in a region of the storm not known for producing GJs (outside of the overshooting top area). For Event #3, the overshooting top region of the storm, located northeast of the storm along the Kansas-Nebraska border, perhaps caused some radar attenuation. This may have been the

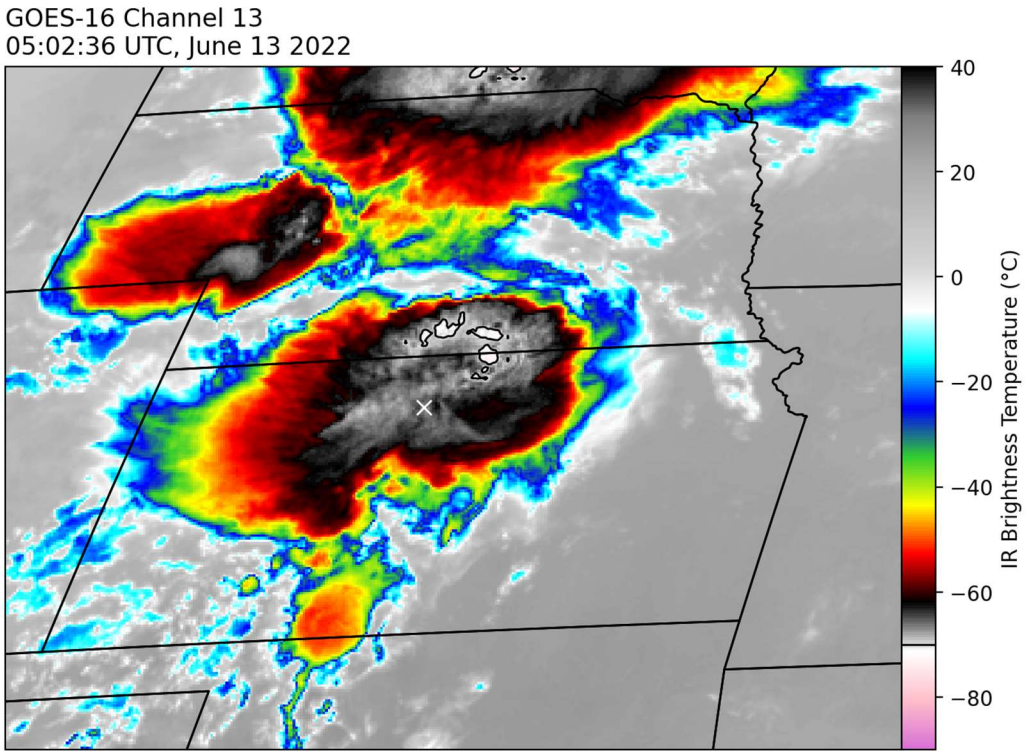

Figure 1. GOES-16 Channel 13 Imagery of the storm complex that produced the GJ. The white 'X' represents the location of Storm A, Event #3 (see Table 1). -70 °C isotherms are also plotted on top of the IR brightness temperature.

reason that it appeared on radar (not shown) that the GJ occurred in an area of relatively low reflectivity. Satellite imagery (seen in Figure 1) offers a different perspective. The GJ occurring in higher clouds, suggested by the colder IR brightness temperatures, matches the results of previous studies (i.e., Lazarus et al. 2015). In comparison to the radar imagery, the satellite imagery suggests a more widely spread system beyond the main convective region.

The ERA5 sounding reveals a nearly well mixed environment closer to the surface, suggesting the presence of afternoon thermals causing mixing. Surface observations (seen in Figure 2) also suggest a dryline in eastern Colorado and eastern Kansas, with dewpoints in the 60s and 70s in western and central Kansas and dewpoints in the 50s in southeastern Colorado. Around 2100 UTC, the storm developed near Two Buttes, Colorado and traveled northeast, following mid-level (500 hPa) and upper-level (300 hPa) winds.

The storm track and environmental conditions (as presented in Figure 3) offer another perspective on the storm's development. Due to the grid spacing of ERA5 reanalysis data, the initial sounding (a) represents an area slightly southwest of the pre-storm environment. All other soundings in Figure 3 also show pre-storm environments, spaced northeast of the storm's location at the same time. As it traveled to the northeast

into central and northern Kansas, the storm had an environment with more moisture allowing for an increase in CAPE. Also of note is that directional wind shear became more favorable for supercell development when going northeast. The only inhibiting factor is the slight inversion at the surface in the latter soundings.

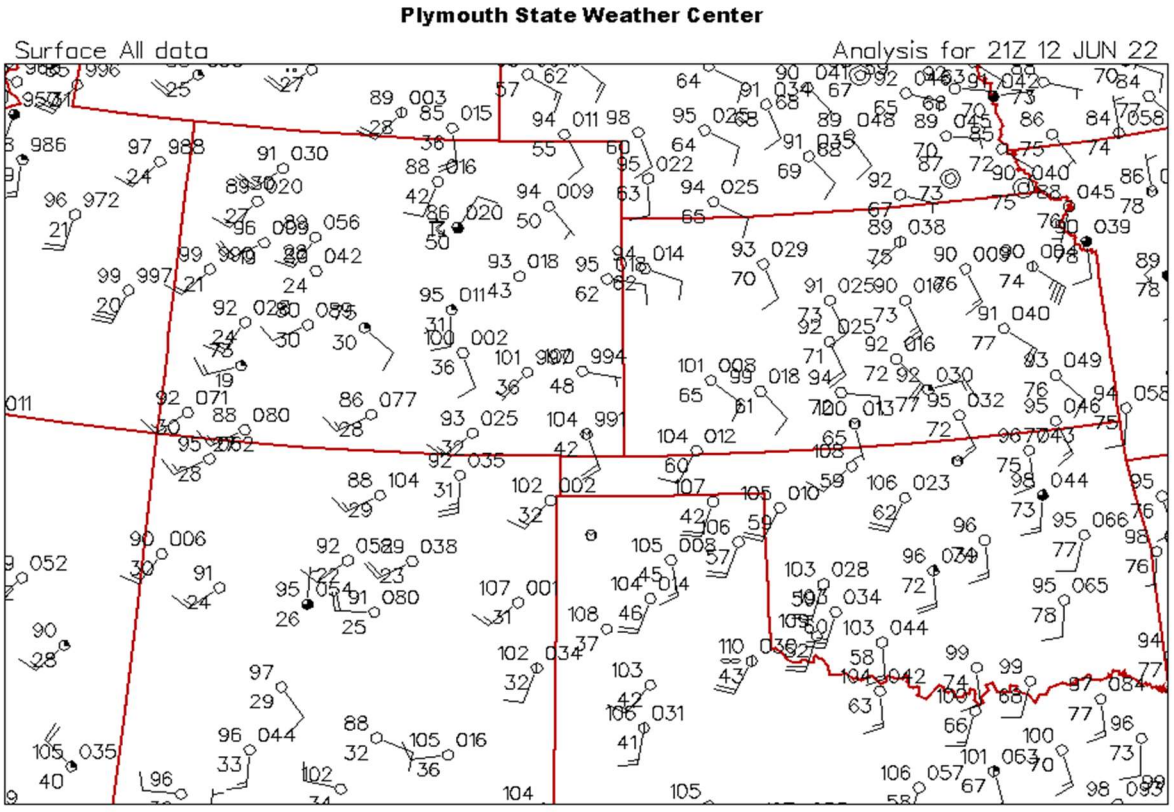

Figure 2. Surface observations at 2100 UTC, before the GJ-producing Storm A developed. Map courtesy of the Plymouth State Weather Center's Make Your Own: Product Generator for Real-Time and Archived data (https://vortex.plymouth.edu/myowxp/).

3.2 Florida GJ-producing storm (Storm B)

This thunderstorm formed under maritime tropical conditions, in stark contrast to the formation of the previously analyzed storm in Kansas. The radar data (Figures 4 and 5) shows an area of prevalent divergence near the storm top. Such storm top divergence confirms the results presented by Lazarus et al. (2015). As seen in the radar imagery, the storm has an overshooting top, about at the location of the GJ. At approximately 14 km, the storm top divergence is prevalent as greater than 15 m s^{-1} winds went towards the radar and 15 m s^{-1} winds headed away from the radar.

3.3 Northern Mexico GJ-producing storm (Storm C)

The Northern Mexico storm's formation environment, compared to the two previous cases, is relatively unremarkable (see Figure 6) and initiated at approximately 0043 UTC on 13 May 2005, near the KDFX NEXRAD radar in south Texas. Perhaps, over a longer time period of analysis, this storm's environmental conditions can be

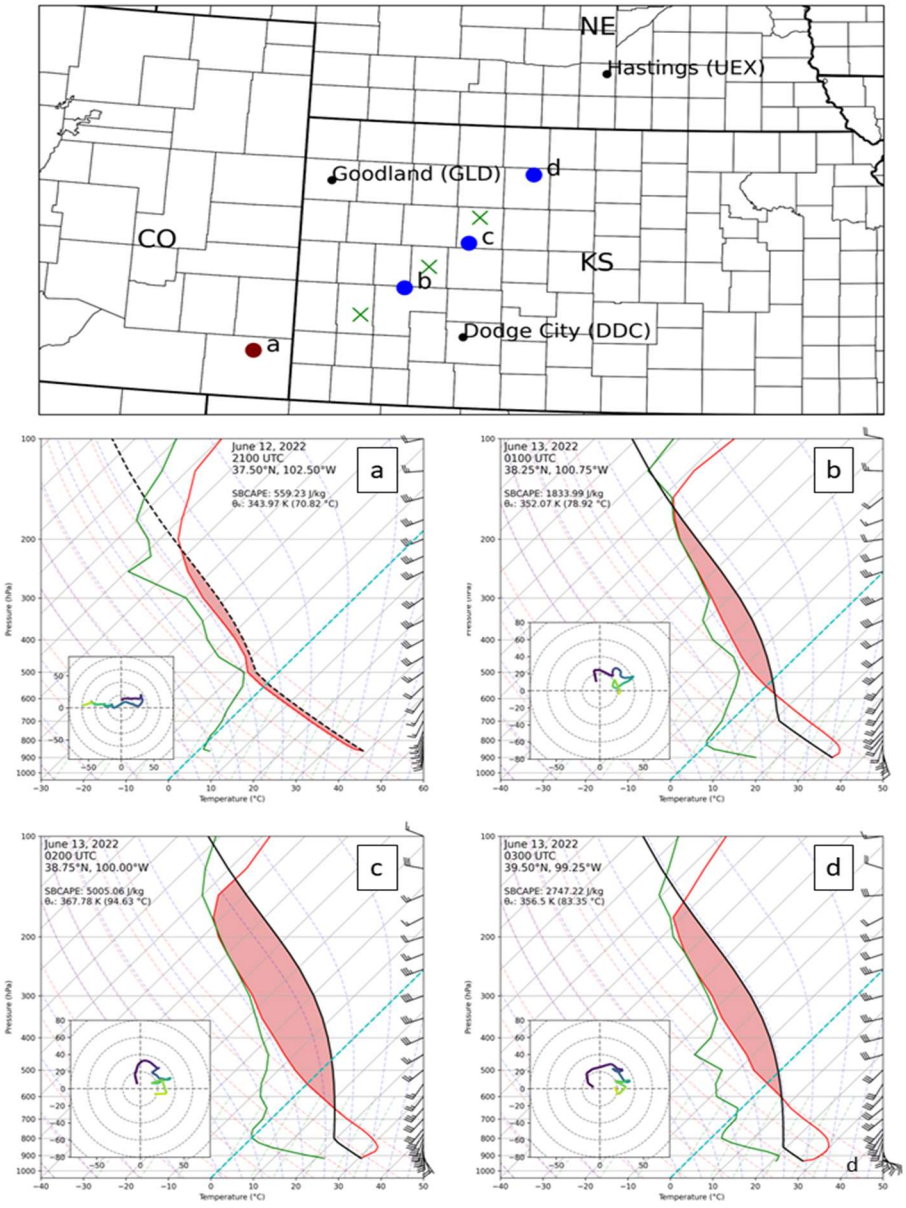

Figure 3. Skew-T log-Ps in a pre-storm environment (Storm A from Table 1). The green 'X's show the storm location before the blue dots representing the sounding location. SBCAPE and surface-based equivalent potential temperature are also given for each sounding location. The 'a' dot is maroon because it represents the storm's initial location.

deduced. The low CAPE, similar to the one presented in van der Velde and Coauthors (2010), provides an interesting contrast to the previously analyzed storms.

Wind veering with height (southeasterly surface winds and southwesterly mid-level winds) suggested warm air advection at the surface. Once enough latent heat is released from the developing thunderstorm, it is more likely that the supercell will

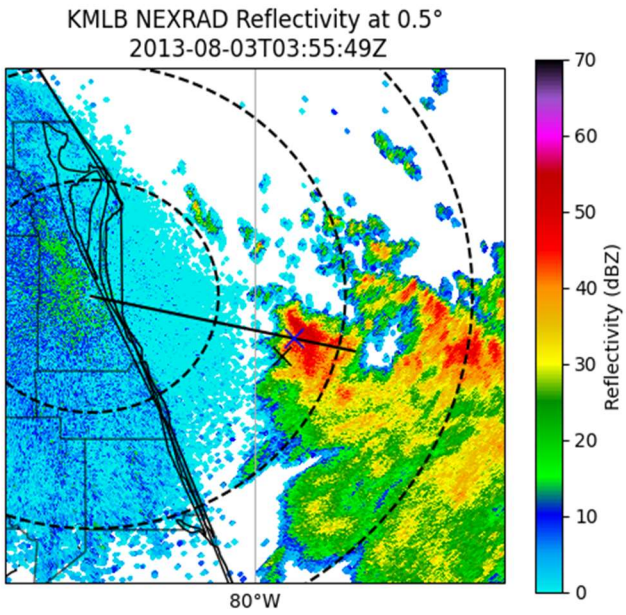

Figure 4. Base reflectivity PPI map taken from KMLB radar. The dashed rings represent range rings at 50, 100, and 150 km. The black solid line going away from the radar represents the azimuth along which the cross section was taken (see Fig. 3). Black 'X' represents the location of Storm B Event #1 (see Table 1), while the Blue 'X' represents the location of Storm B Event #2.

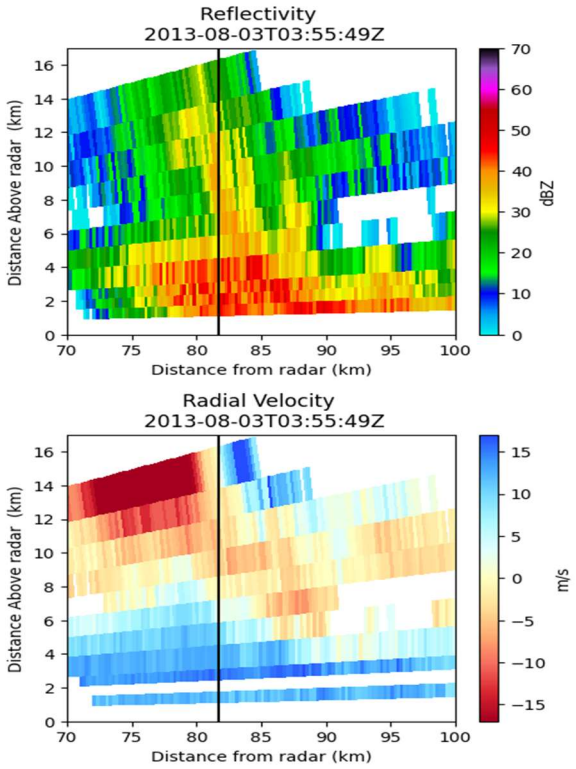

Figure 5. RHI cross section of radar reflectivity and radial velocity at the azimuth of 104.5˚ (see Fig. 2. for radial/azimuth on map) at the approximate time of Storm B Events #1 and #2 (see Table 1). The black line represents the approximate horizontal (distance from the radar) of the GJ.

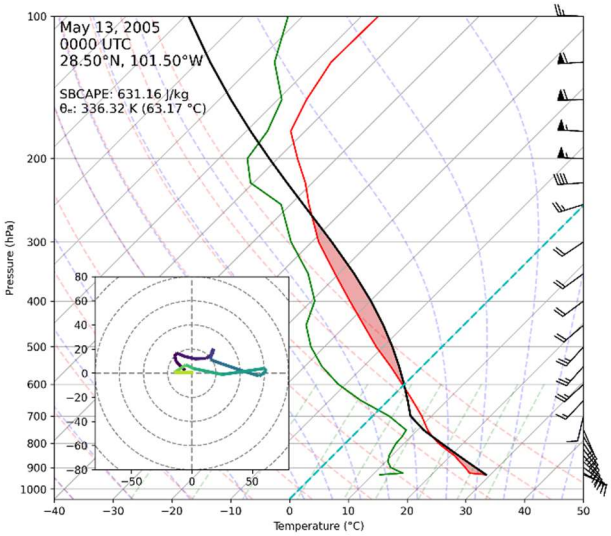

Figure 6. Sounding of the Northern Mexico GJ-producing pre-storm environment. SBCAPE and equivalent potential temperature are stated on the sounding.

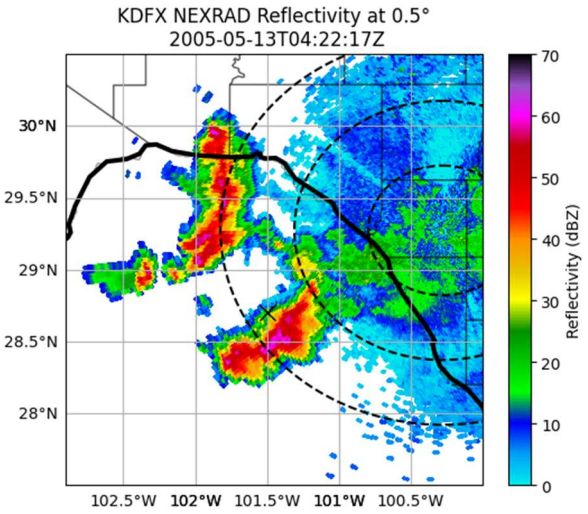

Figure 7. NEXRAD Reflectivity from KDFX at the approximate time of the GJ occurrence. The 'X' marks the approximate location of the GJ.

develop, especially with the amount of shear. Another interesting aspect of this storm is the approximate location of the GJ (see Figure 7) in relation to the overshooting top (away from it, similar to the Kansas storm).

4. Discussion

One alternative interpretation of the Florida GJ-producing storm can be seen in the environment — it developed in the midst of tropical depression Dorian in 2013, as analyzed by Lazarus et al. (2015). Many of the cases presented in section 1 of this paper formed in a tropical maritime environment (see Pasko et al. 2002, Su and Co-authors 2003, and Lazarus et al. 2015) or in tropical cyclones (see Lazarus et al. 2021). From this, it could be assumed that GJs mostly occur in tropical environments. However, this study presented two cases where the storms did not necessarily develop in tropical environments, in particular the Kansas storm. Perhaps one could speculate that while the storm may need an overshooting top or strong convection to produce GJs, the GJ does not need to occur within this same region of the storm, as also seen in the Kansas GJ storm. More methods, such as analyzing shear through specific parameters, utilized in analyzing GJ-producing storms can also provide greater insight into how to diagnose these storms, and perhaps even forecast them. Another variable, the vertical distance between the -10 °C and -50 °C isotherms, as discussed in van der Velde et al. (2022), may also help in diagnosing the storm. Some lingering questions from this study remain unanswered. Is there a general category of storms or mode of convection most common in producing GJs? What differentiates general summer thunderstorms from GJ-producing storms?

5. Conclusions

All GJ-producing thunderstorms exhibited both similar and differing characteristics. The most similar characteristic among the storms was the prevalence of shear in the soundings and radar data. Even though only discussed in one case, the colder IR brightness temperatures presented in the new Kansas GJ cases aligns with previous studies. The differing characteristics shine through the most, however. Two strong cells over land produced GJs, while a maritime tropical storm produced GJs as well. Other differences include high values of equivalent potential temperatures in the Kansas storm, compared to the relatively low equivalent potential temperature in the North Mexico GJ storm. In summary, the atmospheric conditions that allow for the creation of GJ-producing thunderstorms can give insight into the type of storms that produce GJs and the specific environment they occur in.

Given the scope of this research project, a more detailed look into different thermodynamic and dynamic variables could provide a clearer diagnosis of GJ-producing thunderstorms. That said, future research could involve more cases studies, a more statistical approach on comparing cases and their environments, and a higher resolution dataset.

Acknowledgements

The Kansas GJ storm would not have been analyzed without the assistance of Dr. Levi Boggs of the Georgia Tech Research Institute, who provided the location and times of the GJs. A note of sincere appreciation is also extended to Dr. Elaine Godfrey of UNC Asheville for the opportunity to research. I would like to thank every student in the ATMS 464 Scientific Writing class for providing support and peer reviews. I would also like to thank Sharon Withrow for providing continued support and organizing funding for travel reimbursements to present this research.

Data Availability Statement

NOAA NEXRAD data are openly available through NCEI at https://www.ncdc.noaa.gov/nexradinv/map.jsp. All satellite data are available through NOAA and AWS at https://registry.opendata.aws/noaa-goes/ or through the NOAA CLASS server at https://www.aev.class.noaa.gov/saa/products/welcome. ERA5 data can be accessed for free through the Copernicus Climate Data Store at https://cds.climate.copernicus.eu/cdsapp#!/home.

References

Helmus, J. J., and S. M. Collis, 2016: The Python ARM Radar Toolkit (Py-ART), a library for working with weather radar data in the Python programming language. *J. Open Res. Software,* **4,** e25, https://doi.org/10.5334/jors.119.

Hersbach, H., and Coauthors, 2020: The ERA5 global reanalysis. *Quart. J. Roy. Meteor. Soc.,* **146,** 1999–2049, https://doi.org/10.1002/qj.3803.

Lazarus, S. M., M. E. Splitt, J. Brownlee, N. Spiva, and N. Liu, 2015: A thermodynamic, kinematic, and microphysical analysis of a jet and gigantic jet-producing Florida thunderstorm. *J. Geophys. Res. Atmos.,* **120,** 8469–8490, https://doi.org/10.1002/2015JD023383.

——, J. Chiappa, H. Besing, M. E. Splitt, and J. A. Riousset, 2021: Distinguishing characteristics of the tropical cyclone gigantic jet environment. *J. Atmos. Sci.,* **78,** 2741–2761, https://doi.org/10.1175/JAS-D-20-0265.1.

Meyer, T. C., T. J. Lang, S. A. Rutledge, W. A. Lyons, S. A. Cummer, G. Lu, and D. T. Lindsey, 2013: Radar and lightning analyses of gigantic jet-producing storms. *J. Geophys. Res. Atmos.,* **118,** 2872–2888, https://doi.org/10.1002/jgrd.50302.

Pasko, V. P., M. A. Stanley, J. D. Matthews, U. S. Inan, and T. G. Wood, 2002: Electrical discharge from a thundercloud top to the lower ionosphere. *Nature,* **416,** 152–154, https://doi.org/10.1038/416152a.

Su, H. T., and Coauthors, 2003: Gigantic jets between a thundercloud and the ionosphere. *Nature,* **423,** 974–976, https://doi.org/10.1038/nature01759.

van der Velde, O. A., W. A. Lyons, T. E. Nelson, S. A. Cummer, J. Li, and J. Bunnell, 2007: Analysis of the first gigantic jet recorded over continental North America. *J. Geophys. Res.,* **112,** D20104, https://doi.org/10.1029/2007JD008575.

——, and Coauthors, 2010: Multi-instrumental observations of a positive gigantic jet produced by a winter thunderstorm in Europe. *J. Geophys. Res.,* **115,** D24301, https://doi.org/10.1029/2010JD014442.

——, J. Montanyà, J. A. López, and S. A. Cummer, 2019: Gigantic jet discharges evolve stepwise through the middle atmosphere. *Nat. Comm.,* **10,** 4350, https://doi.org/10.1038/s41467-019-12261-y.

——, J. Montanyà, and J. A. López, 2022: Meteorological factors in the production of gigantic jets by tropical thunderstorms in Colombia. Atmos. Res., 277, 106 316, https://doi.org/10.1016/j.atmosres.2022.106316.